Atmospheric
Chemistry
and Physics

Open Access

EGU

Supplement of

Optical properties of meteoric smoke analogues

Tasha Aylett et al.

Correspondence to: John M. C. Plane (j.m.c.plane@leeds.ac.uk)

Contained in this SI is the following:

Figure S1. Schematic diagram of the TRAPS apparatus, including the MICE. Image modified from Nachbar et al. (2018).

Figure S2. Average particle mass as a function of residence time in the MICE, for experimental runs under one set of conditions (supersaturation, initial particle mass)/ Irradiation of particles at 0 mW (black) 5 mW (blue) 10 mW (purple) and 15 mW (brown).

Figure S3. TEM electron diffraction pattern of an iron oxide agglomerate particle produced in the photochemical reactor, showing the intense reflections of maghemite or possibly oxide-coated magnetite.

Figure S4. EDX spectrum of the iron oxide particles produced in the photochemical reactor.

Table S1. Absorption cross section of $Fe(CO)_5$ at 293 K.

Table S2. Functions used to fit to generate imaginary refractive indices from the best-fit real refractive indices at 405, 488 and 660 nm (1-3), and the function used to define the wavelength dependence of the imaginary refractive index using values defined from best-fit data at 405, 488 and 660 nm (4).
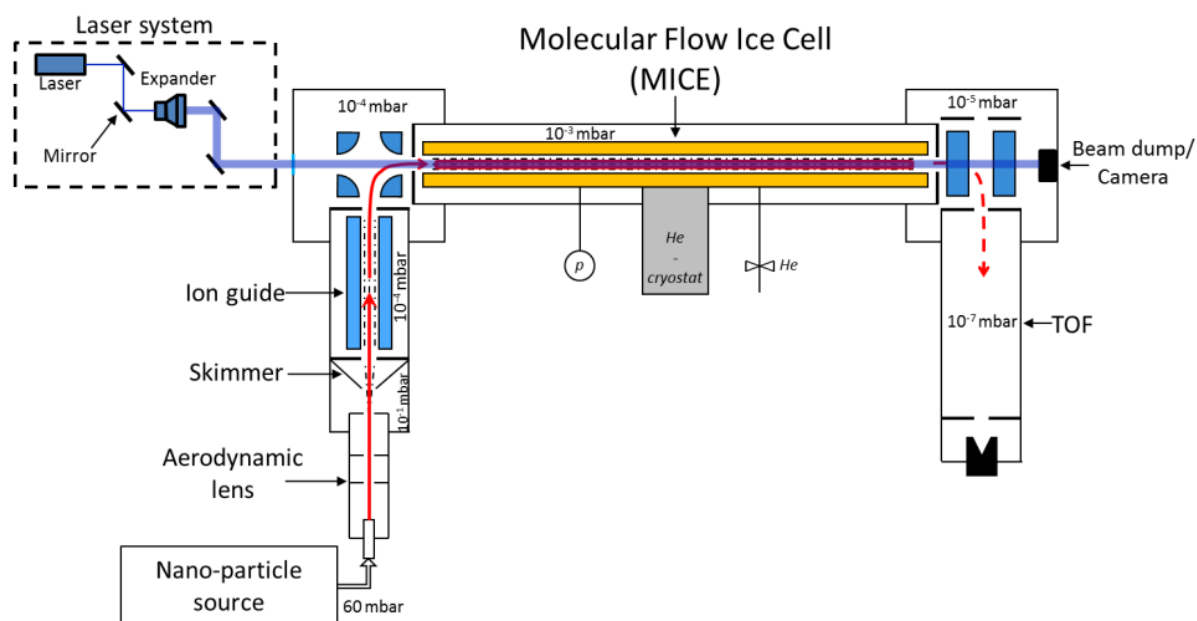
Figure S1. Schematic diagram of the TRAPS apparatus, including the MICE. Image modified from Nachbar et al. (2018).
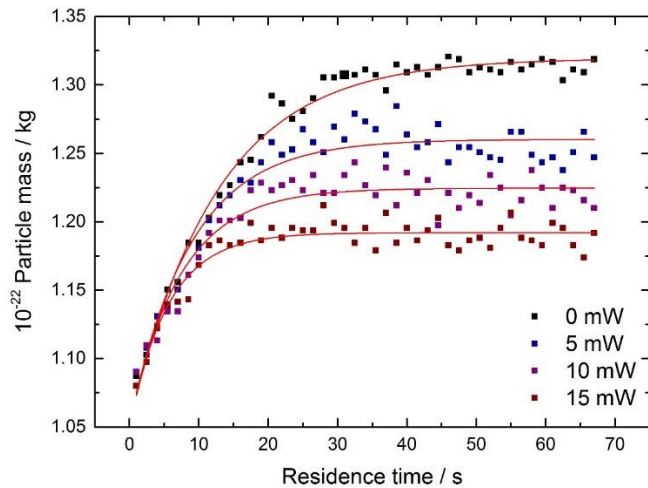
Figure S2. Average particle mass as a function of residence time in the MICE, for experimental runs under one set of conditions (supersaturation, initial particle mass)/ Irradiation of particles at 0 mW (black) 5 mW (blue) 10 mW (purple) and 15 mW (brown).
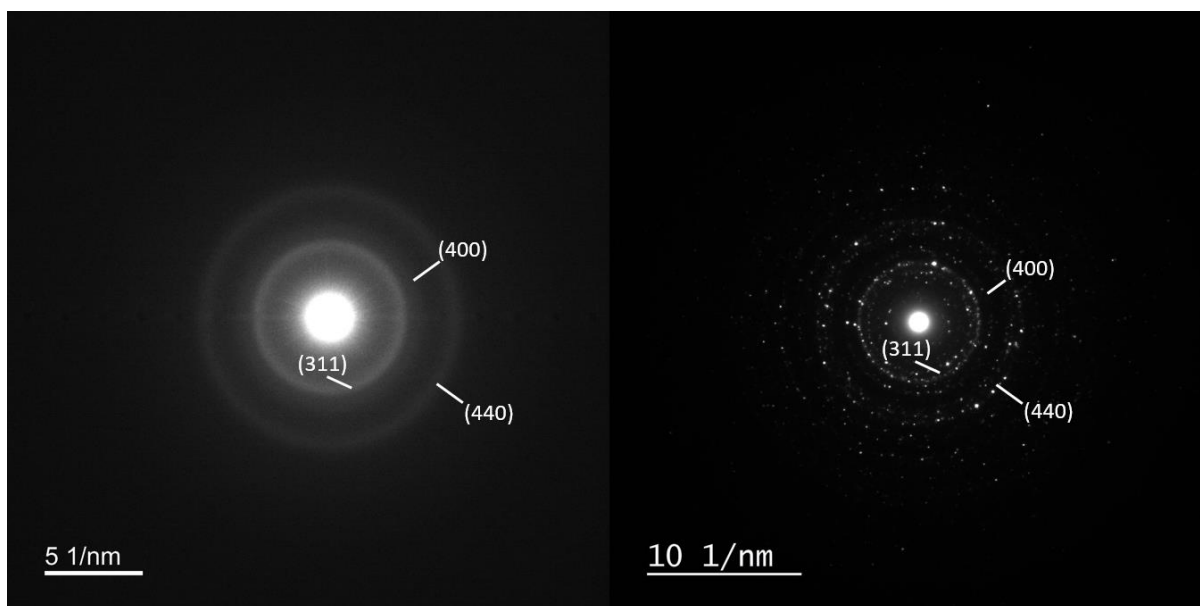
Figure S3. Left panel: TEM electron diffraction pattern of an iron oxide agglomerate, showing the intense reflections close to the 311, 400 and 440 diffraction planes. Right panel: Electron diffraction pattern for a maghemite standard.
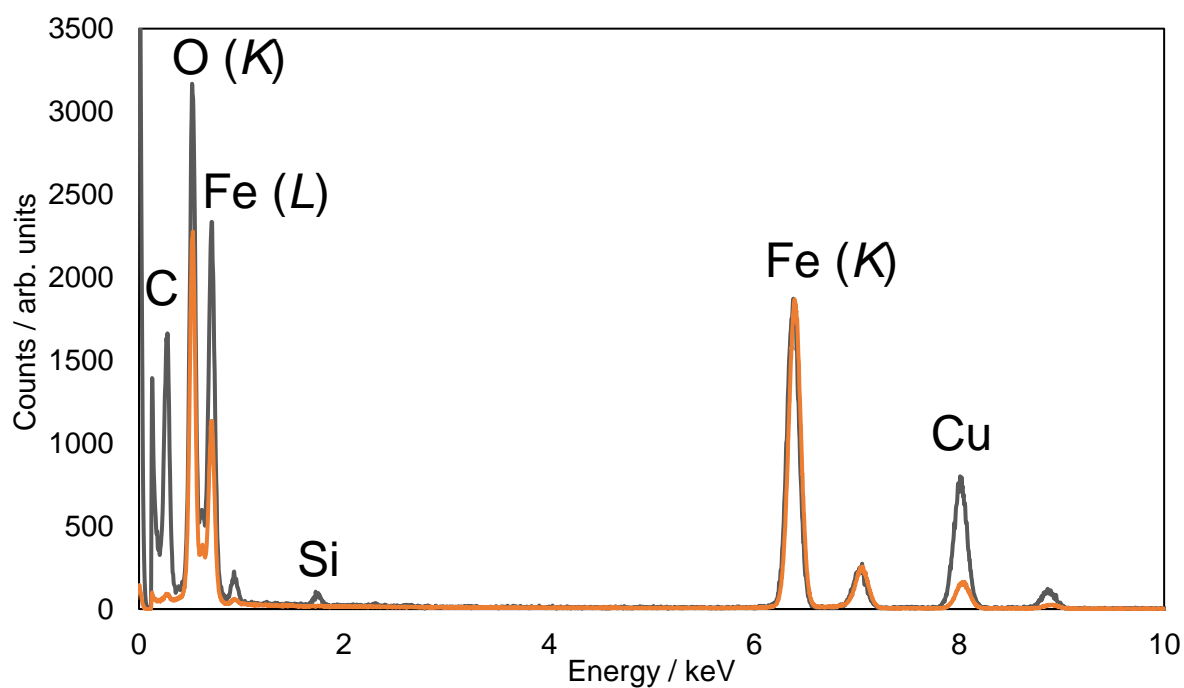
Figure S4. EDX spectrum of the iron oxide agglomerates produced in the photochemical reactor (grey) and an equivalent spectrum for a maghemite standard (orange). The spectrum for the maghemite standard has been scaled for clarity.

Table S1. Absorption cross section of Fe(CO)$_5$ at 293 K.

Wavelength /nm	Absorption Cross section / cm^2	Wavelength /nm	Absorption Cross section / cm^2
190	3.14×10^{-17}	450	1.95×10^{-20}
200	3.96×10^{-17}	460	1.76×10^{-20}
210	2.63×10^{-17}	470	1.65×10^{-20}
220	1.62×10^{-17}	480	1.57×10^{-20}
230	1.30×10^{-17}	490	1.45×10^{-20}
240	1.23×10^{-17}	500	1.39×10^{-20}
250	1.12×10^{-17}	510	1.33×10^{-20}
260	8.38×10^{-18}	520	1.29×10^{-20}
270	5.89×10^{-18}	530	1.23×10^{-20}
280	4.47×10^{-18}	540	1.18×10^{-20}
290	2.94×10^{-18}	550	1.15×10^{-20}
300	1.75×10^{-18}	560	1.09×10^{-20}
310	1.01×10^{-18}	570	1.04×10^{-20}
320	6.20×10^{-19}	580	1.01×10^{-20}
330	4.21×10^{-19}	590	9.87×10^{-21}
340	3.23×10^{-19}	600	9.40×10^{-21}
350	2.63×10^{-19}	610	9.14×10^{-21}
360	2.14×10^{-19}	620	8.69×10^{-21}
370	1.69×10^{-19}	630	8.61×10^{-21}
380	1.27×10^{-19}	640	8.42×10^{-21}
390	9.14×10^{-20}	650	7.97×10^{-21}
400	6.46×10^{-20}	660	7.96×10^{-21}
410	4.59×10^{-20}	670	7.64×10^{-21}
420	3.40×10^{-20}	680	7.30×10^{-21}
430	2.66×10^{-20}	690	7.35×10^{-21}
440	2.22×10^{-20}	700	7.07×10^{-21}

Table S2. Functions used to fit to generate imaginary refractive indices from the best-fit real refractive indices at 405, 488 and 660 nm (1-3), and the function used to define the wavelength dependence of the imaginary refractive index using values defined from best-fit data at 405, 488 and 660 nm (4).

	Wavelength / nm	Function
1	405	$y = y_0 + a_1 \cdot e^{(-x/t_1)} + a_2 \cdot e^{(-x/t_2)}$ Where $y_0 = 0.121$, $a_1 = 1 \times 10^{-29}$, $t_1 = 0.0508$, $a_2 = 0.0337$, $t_2 = 0.850$
2	488	$y = a \cdot e^{(-x/t)} + m \cdot x + c$ Where $a = 0.300$, $t = -2.73$, $m = -0.242$, $c = -0.135$
3	660	$y = a \cdot e^{(-x/t)} + m \cdot x + c$ Where $a = 0.0563$, $t = -3.10$, $m = -0.0482$, $c = -0.0220$
4	350-660	$y = a \cdot b^x$ Where $a = 238$, $b = 0.986$

References

Nachbar, M., Duft, D., Kiselev, A., and Leisner, T.: Composition, Mixing State and Water Affinity of Meteoric Smoke Analogue Nanoparticles Produced in a Non-Thermal Microwave Plasma Source, Zeit. Phys. Chem., 232, 635-648, 2018.